Food Bioprocess Technol (2016) 9:1937–1950
DOI 10.1007/s11947-016-1777-z

ORIGINAL PAPER

Structure, Functionality, and Active Release of Nanoclay–Soy Protein Films Affected by Clove Essential Oil

Ignacio Echeverría[1] · M. Elvira López-Caballero[2] · M. Carmen Gómez-Guillén[2] · Adriana N. Mauri[1] · M. Pilar Montero[2]

Received: 5 April 2016 / Accepted: 10 July 2016 / Published online: 1 August 2016

Abstract Nowadays, there is a pronounced interest in the potential use of biopolymer/layered silicate systems as active food packaging. This manuscript studied the effect of clove essential oil addition to soy protein–montmorillonite (MMT) films on the material's structure, functionality, and active release. Active nanocomposite films were prepared by casting from aqueous dispersions containing soy protein isolates (SPI), glycerol, different concentrations of MMT and clove essential oil. Besides the important antioxidants and antimicrobial properties provided to nanocomposite films, the addition of clove essential oil exerted a plasticizing effect, which was verified in a decrease in the tensile strength and elastic modulus (up to 50 and 75 %, respectively) and an increase of the water content of films (up to 20 %). But the nanoclay caused a further strengthening effect in films containing CEO. While nanocomposite films containing 10 g MMT/100 g SPI reached an increase of 105 and 200 % in tensile strength and Young's modulus, respectively, and a decrease of 340 % in their elongation at break, those that also contained CEO reached higher variations (230, 345, and 290 %, respectively). Clove essential oil presence also favored the exfoliation of montmorillonite into the soy protein matrix, while the nanoclay seemed to promote the release of active compounds, occasionally modifying the antimicrobial activity of films as well as the release of some of its Si and Al ions after being in contact with water (at least twice).

Keywords Active packaging · Soy protein–montmorillonite nanocomposite films · Soy protein films · Clove essential oil in films · Metal release from MMT nanocomposite films · Active release from nanocomposite films

Introduction

One of the most interesting advantages of biopolymers based materials is that they can be used as vehicles for additives such as antioxidants or antimicrobial compounds, vitamins, flavors, colorants, and salts in order to increase its functionality, improve their appearance, and extend the shelf life of foods that can protect (Gómez-Estaca et al., 2010; Han & Gennadios, 2005; Han & Krochta, 2007; Sultanbawa, 2011). The current trend to formulate these active materials is to incorporate natural additives, including some essential oils, such as garlic, lavender, sage, oregano, pepper, thyme, rosemary, and clove (Kong et al., 2007; Kuorwel et al., 2011; Sánchez-González et al., 2011; Seydim & Sarikus, 2006; Yildirim et al., 2000). The advantage of using such essential oils incorporated into the films, rather than applying them directly on the food, is the possibility to achieve the desired target with lower concentrations of oil, thereby avoiding conferring undesirable aromas and flavors to foods (Gutierrez et al., 2009; Sánchez-González et al., 2010). In particular, clove essential oil (*Syzygium aromaticum L.*) mainly contains eugenol, which is an effective inhibitor of the growth of *Listeria monocytogenes*, *Campylobacter jejuni, Salmonella enteritidis, Escherichia coli* and *Staphylococcus aureus* in several culture media (Cressy et al., 2003; Mytle et al., 2006; Velluti et al., 2003).

✉ Adriana N. Mauri
anmauri@quimica.unlp.edu.ar

[1] Centro de Investigación y Desarrollo en Criotecnología de Alimentos (CIDCA), CCT- La Plata. CONICET - Universidad Nacional de La Plata (UNLP), 47 and 116, 1900 La Plata, Buenos Aires, Argentina

[2] Instituto de Ciencia y Tecnología de Alimentos y Nutrición (ICTAN, CSIC), Calle José Antonio Novais, 10, 28040 Madrid, Spain

Its addition to biopolymer films has been studied (Gómez-Estaca et al., 2010; Salgado et al., 2013).

Nowadays, there is a pronounced interest in the potential use of biopolymer/layered silicate systems as food packaging (Kumar et al., 2010; Azevedo et al., 2015) Nanoclays dispersed into the biopolymer matrix besides improving the mechanical and barrier properties of the resulting films, could also modify the release of active compounds present in the formulation. The possibility of achieving control release of certain compounds through the addition of nanoreinforcements to a polymeric matrix is shown as an interesting strategy that is being studied. Mascheroni et al. (2010) developed a delivery system for carvacrol in a wheat gluten matrix reinforced with montmorillonite (MMT) that was clearly effective in retaining and protecting the active antimicrobial agent during the processing stage. Quilaqueo Gutiérrez et al. (2012) studied the functionality of nanocomposite films based on carboxymethylcellulose-montmorillonite (CMC-MMT) activated with myrtle extract. They showed that the extract besides conferring important antioxidant properties to nanocomposite films modified the ratio of permeability to different gases (O_2 and CO_2), and suggested that clays in these films could modulate the release of active compounds. In this regard Giménez et al. (2012) found that the incorporation of sepiolite in gelatin and egg white protein films activated with clove essential oil, increased the release of eugenol and also some protein components, which meant a controlled release of the antioxidant activity as well as a greater antimicrobial activity.

But as the addition of a bioactive compound into a material formulation is no guarantee to obtain an active packaging, the presence of certain nanoreinforcement can not ensure the control release of the active compounds in any direction (increasing or decreasing the rate of its release). Possible interactions that may arise among the various components of the formulation during film formation, would affect the potential release or retention of active ingredients, thus affecting their final activity. Even the determination of a certain activity by an in vitro technique does not ensure that the container can gain the ability to protect the food during storage (Salgado et al., 2015).

In a previous work (Echeverría et al., 2014), the preparation of soy protein–MMT nanocomposite film was studied. Important improvements in the mechanical properties of soy protein films and in their resistance to water were observed upon inclusion of MMT in the formulation that were likely related to the degree of intercalation and consequent exfoliation of the clay layers in the protein matrix. This propitious restructuring of the admixture of soy protein and MMT, in turn, could be attributed to the beneficial interactions generated between the MMT and the soy protein within the films. The uniform dispersion of the laminas of clay within the matrix increased the area of protein–clay contact and further contributed to the efficient functionality of these nanocomposite films, demonstrating that MMT could act as a major strengthening component when added to soy protein films. The clay also modifies protein–protein, protein–glycerol, protein–water, and glycerol–water interactions, as it was demonstrated by differential solubilization of proteins in the nanocomposites films.

Taking into account that the activation of nanocomposite films based on soy protein isolates-MMT with essential oils has not been previously analyzed, the aim of the present work was to study the effect of clove essential oil addition to soy protein–MMT nanocomposite film structure, functionality, and active release.

Materials and Methods

Materials

Soy protein isolate (SPI; SUPRO 500-E) was generously provided by The Solae-Company (Brazil). The protein content of SPI, as measured by the Kjeldahl method, was 85 ± 2 % (*w*/*w*, dry weight; $N \times 6.25$). Clove essential oil (*S. aromaticum* L.) (CEO; Eladiet SA., Spain) was used to activate the films. Sodium MMT without organic modification (Cloisite®Na^+) was supplied by Southern Clay Products (USA). It has a cation-exchange capacity of 92.6 meq/100 g clay, a typical interlayer distance of 11.7 Å, a bulk density of 2.86 g ml^{-1}, and a typical particle-size distribution between 2 and 13 μm. Glycerol (p.a., Anedra, Argentina) was used as a film plasticizer.

Film Preparation

Films were prepared by casting taking into account the results of previous studies (Echeverría et al., 2014; and Salgado et al., 2013). Five grams of SPI was dispersed in 80 ml of distilled water at room temperature by magnetic stirring and the pH of the dispersion adjusted to 10.5 with 2 N NaOH. Different amounts of MMT powder (0, 0.25 and 0.5 g) plus 1.25 g of glycerol were likewise dispersed in 20 ml of distilled water followed by sonication (Sonics & Materials Inc., Sonics Vibra-cell model VCX 130, USA) at 80 % amplitude. Then SPI-glycerol dispersion and MMT suspension were mixed under magnetic stirring for 1 h at room temperature and 0.5 ml of clove essential oil (CEO) was added, and the last dispersion was mixed 30 more minutes. Finally, 10 ml of film-forming dispersions were cast onto polystyrene Petri dishes (144 cm^2) and dried in an oven (Binder FD240, Germany) at 60 °C for 3 h. Before any tests were performed, the films were preconditioned at 20 °C and 58 % relative humidity (RH) for 48 h. Three MMT contents were studied: 0, 5, and 10 g MMT/100 g SPI, with or without CEO.

Characterization of Films

Film Thickness

Before testing, the film thickness was measured by a digital micrometer (Mitutoyo, model MDC-25 M, Japan). Measurements were done at five positions along the rectangular strips for the tensile test, and at the center and at eight positions round the perimeter for the WVP determinations. The mechanical properties and WVP were calculated using the average thickness for each film replicate.

Moisture Content

Small specimens of films (≈0.25 g) were collected after conditioning, cut, and weighed before and after drying in an oven at 105 °C for 24 h. Moisture content values were determined in triplicate as the difference between the two weights for each film and were expressed as a percent of the original weight (American Society for Testing and Measurements [ASTM] D644–94, ASTM E96-00, 1996).

Opacity

Each film specimen was cut into a rectangular piece and placed directly in a spectrophotometer cell, and measurements were performed with air as the reference for transparency. A spectrum of each film was obtained in a UV–Vis spectrophotometer (Shimadzu UV-1601, model CPS-240, Japan). The area under the absorption curve from 400 to 800 nm was recorded and the opacity of the film (arbitrary units/mm) calculated by dividing the absorbance at 500 nm by the film's thickness (Cao et al., 2007). All determinations were performed in triplicate.

Film Color

Films color was determined using a Minolta Chroma meter (Minolta Chroma Co., CR 300, Japan). A CIE Lab color scale was used to measure the degree of lightness (L), redness (+a) or greenness (−a), and yellowness (+b) or blueness (−b) of the films. The instrument was standardized by means of a set of three Minolta calibration plates. The films were measured on the surface of the white standard plate with color coordinates of $L = 97.3$, $a = 0.14$ and $b = 1.71$. Total color difference (ΔE) was calculated from:

$$\Delta E = \sqrt{(L_{film} - L_{standard})^2 + (a_{film} - a_{standard})^2 + (b_{film} - b_{standard})^2} \quad (1)$$

Values were expressed as the means of nine measurements on different areas of each film.

Water Vapor Permeability

Water vapor permeability (WVP) tests were conducted by the ASTM method E96–00 (ASTM E96-00, 1996) with certain modifications (Gennadios et al., 1994). Each film sample was sealed over a circular opening of 0.00159 m^2 in a permeation cell that was subsequently stored at 20 °C in a desiccator. To maintain a 75 % RH gradient across the film, anhydrous silica (0 % RH_c) was placed inside the cell and a saturated NaCl solution (75 % RH) in the desiccator. The RH therefore was always lower inside the cell than outside, and the water vapor transport was accordingly determined from the weight gain of the permeation cell. When steady-state conditions were reached (after about 1 h), eight weight measurements were made over a period of 7 h. Changes in the weight of the cell were recorded and plotted as a function of time. The slope of each line was calculated by linear regression (Origin Pro 8.5 software), and the water vapor–transmission rate was calculated from the slope (g H_2O s^{-1}) divided by the cell area (m^2). WVP (g H_2O/Pa.s.m) was calculated as:

$$WVP = \frac{WVTR}{P_v^{H_2O} \cdot (RH_d - RH_c) \cdot A} \quad (2)$$

Where WVTR = the water vapor–transmission rate, $P_v^{H_2O}$ = vapor pressure of water at saturation (1753.35 Pa) at the test temperature (20 °C), RH_d = RH in the desiccator, RH_c = RH in the permeation cell, A = permeation area, and d = film thickness (m). Each WVP value represents the mean value of at least three samples taken from different films.

Solubility

The solubility of films was determined in triplicate, according to the method proposed by Gontard et al. (1993). Three pieces of film (2 cm in diameter) were immersed in 50 ml distilled water, and the system was slowly stirred at 20 °C for 24 h (with 0.02%*w*/*v* sodium azide). After filtration of the samples (Whatman 1), the non-solubilized material on the paper was dried in a forced-air oven (105 °C, 24 h) in order to determine the weight of the water-insoluble fraction as a percent of the total.

Mechanical Properties

The tensile strength, Young's modulus, and elongation at break of the films were determined following the procedures outlined in the ASTM methods D882–91 with an average of six measurements taken for each film and with at least two films per formulation. The films were cut into 6-mm by 80-mm strips that were mounted between the grips of the texture analyzer (Stable Micro Systems, TA.XT2i, England). The initial grip separation was set at 50 mm and the crosshead speed

at 0.5 mm/s. The tensile strength (σ = force per initial cross-sectional area) and elongation at break (ε) were determined directly from the stress–strain curves through the use of OriginPro 8 SR0 v8.0724 software (OriginLab Corporation, USA), and the Young's modulus (E) was obtained from the slope of the initial linear portion of that curve.

X-ray Diffraction

X-ray diffraction was carried out on a Bruker D8 Advance (Bruker GbmH, Germany) equipped with a Cu Kα radiation source (λ = 0.154 nm). The voltage and the current used were 40 kV and 40 mA, respectively. The diffraction data—expressed as intensity (A.U.)—were collected from 2θ = 1.5–10° in a fixed-time mode with a step interval of 0.01°. The basal spacing of the silicate layer, *d*, was calculated by means of the Bragg equation:

$$\lambda = 2d \ \sin\theta \tag{3}$$

where θ is the diffraction position and λ is the wavelength.

Antioxidant Properties

The antioxidant activity of the supernatants obtained in a solubility test (2.3.9) of the resulting protein and nanocomposite films were characterized by its radical scavenging ability (ABTS assay) and its ferric ion reducing capacity (FRAP assay). The ABTS radical (2, 20-azinobis-(3-ethylbenzothiazoline-6-sulfonic acid)) scavenging capacity released after 16 h was determined according to a modified version of the method of Re, et al. (1999). The stock solution of ABTS radical consisted of 7 mM ABTS (Sigma-Aldrich) in potassium persulfate 2.45 mM (Sigma-Aldrich), kept in the dark at room temperature for 12 to 16 h. An aliquot of the stock solution was diluted with distilled water in order to prepare the working solution of ABTS radical with absorbance at 734 nm of 0.70 ± 0.02 (Shimadzu UV-1601, model CPS-240, Japan). A 20 μl aliquot of the samples was mixed with 980 μl of ABTS reagent. The mixture was then left to stand at 30 °C for 10 min and the absorbance values were read at 734 nm. Results were expressed as milligrams of ascorbic acid per gram of soluble film based on a standard curve of vitamin C (Sigma-Aldrich), which relates the concentration of vitamin C to the amount of absorbance reduction caused by vitamin C. All determinations were performed at least in triplicate.

FRAP (ferric-reducing ability of plasma) is a measure of the reducing ability of samples and was performed according to the method described by Pulido et al. (2000). Samples (30 μL) were incubated (37 °C) with 90 μL of distilled water and 900 μL of FRAP reagent (containing 2,4,6-tris(2-pyridyl)-s-triazine (TPTZ, Sigma-Aldrich) and $FeCl_3$). Absorbance values were read at 595 nm after 30 min. Results were expressed as mmol $FeSO_4.7H_2O$ equivalents/g of soluble film based on a standard curve which relates its concentration to the absorbance at 595 nm. All determinations were carried out in triplicate.

Total Phenolic Content

Polyphenols were quantified spectrophotometrically at 750 nm (Shimadzu UV-1601, model CPS-240, Japan) using the Folin-Ciocalteu reagent and gallic acid as standard (Montreau, 1972). Results were expressed as mg of galic acid/g of soluble film. All determinations were performed at least in triplicate.

Antimicrobial Properties

The antimicrobial activity of the protein and nanocomposite films was determined by the agar diffusion method against 26 microorganisms as previously described (Arancibia et al., 2015). Briefly, edible films were cut into disks of a 30-mm diameter and laid onto the surface of agar previously inoculated with 100 μL of each microorganisms. The strains, selected by its importance in health (such as probiotics or pathogens) or for being responsible for food spoilage, were obtained from the Spanish Type Culture Collection (CECT) and the Leibniz Institute DSMZ (Germany): *Aeromonas hydrophila* CECT 839T, *Aspergillus niger* CECT 2088, *Bacillus cereus* CECT 148, *Bacillus coagulans* CECT 56, *Bifidobacterium animalis* subespecie *lactis* DSMZ 10140, *Bifidobacterium bifidum* DSMZ 20215, *Brochothrix thermosphacta* CECT 847, *Citrobacterfreundii* CECT 401, *Clostridium perfringens* CECT 486, *Debaryomyceshansenii* CECT 11364, *Enterococcus faecium* DSM 20477, *Escherichia coli* CECT 515, *Lactobacillus acidophilus* CETC 903, *Lactobacillus helveticus*DSM 20,075, *Listeria innocua* CECT 910, *Listeria monocytogenes* CECT 4032, *Penicilium expansum* DSMZ 62841, *Photobacterium phosphoreum* CECT 4192, *Pseudomonas aeruginosa* CECT 110, *Pseudomonas fluorescens* CECT 4898, *Salmonella cholerasuis* CECT 4300 *Shewanella putrefaciens* CECT 5346 T, *Shigella sonnei* CECT 4887 *Staphylococcus aureus* CECT 240, *Vibrio parahaemolyticus* CECT 511 T, *Yersinia enterocolitica* CECT 4315. All the strains were grown in BHI broth (Oxoid, UK) (supplemented with 3 % NaCl for *V. parahaemolyticus* and 1 % NaCl for *P. phosphoreum*). Organisms were incubated at 37 °C excepting *A. hydrophila*, *P. fluorescens*, *S. putrefaciens*, incubated at 30 °C; *B. thermosphacta* at 25 °C and *P. phosphoreum* at 15 °C. In addition, *L. acidophilus* was incubated under CO_2 flow and *C. perfringens* under anaerobic conditions (Gas-Pack, Anaerogen; Oxoid). After incubation, the inhibition (clear) area—considered the antimicrobial activity—was measured with Corel Photo Paint X3 software. Results were expressed

as percentage of growth inhibition respecting to the total plate surface. Each determination was performed in duplicate.

Transmission Electron Microscopy (TEM)

Small pieces of film (0.5 mm^2) were fixed in 2.5 % (*v*/*v*) glutaraldehyde in Sorenssen buffer (pH 7.2), washed in the same buffer three times for 30 min each, and then postfixed in 2 % (*w*/*v*) OsO_4 for 1 h. The samples were next washed with distilled water three times for 30 min each, serially dehydrated in aqueous acetone (25, 50, 75, and 100 % [3×]), and finally embedded in Spurr Resin and epoxi resin (1:2, 2:2, 2:1) overnight. Polymerization was carried out at 50 °C during 120 h. The embedded samples were sectioned with an Reichert-Jung Ultracut-K ultramicrotome. The grids were stained with uranyl acetate (1 min) and lead-citrate (40 min) and observed with a transmission electron microscope (JEOL JEM 2100, Japan) at 200 kV.

Determination of Metals

The supernatants obtained in the solubility test (2.3.9) were used for testing the metal release from the nanocomposites films. These samples (2 ml) were digested in triplicate in a Microwave Digestion LabStation (Milestone Inc., model Ethos 1, USA). Digestion was performed in closed vessels made of high-density Teflon TFM, using nitric acid (8 ml) and hydrogen peroxide (2 ml) as reagents (PA, Panreac Chemistry, S.A., Barcelona, Spain). Once digested, samples were diluted with ultrapure deionized water (18.2 MW-cm resistivity at 25 °C) (Millipore, Bedford, MA, USA).

Magnesium and sodium were determined by atomic spectroscopy, using an Atomic Absorption Spectrophotometer Perkin-Elmer, mod. Zeeman PC 5100 (Perkin-Elmer, 761 Main Ave., Norwalk, CT 06859–0010—USA), with air–acetylene flame. For magnesium, a hollow cathode lamp was used, and sodium was determined without using lamp (mode emission spectroscopy). Aluminum and silicon were determined with an optical emission spectrometer plasma (ICP-OES), mod. 4300 DV (Perkin-Elmer 761 Main Ave, Norwalk, CT 06859–0010—USA). Each element was determined separately with a calibration curve at different concentrations from 0.01 mg/L upwards, prepared from commercial patterns (Panreac). The limit of detection was 0.01 mg/L.

Statistical Analysis

Results were expressed as mean ± standard deviation and were analyzed by analysis of variance (ANOVA). Means were tested with the Tukey's HSD (honestly significant difference) test for paired comparisons, at a significance level $p < 0.05$, through the use of the Origin Pro 8.5 SR0 v8.0724 software (OriginLab Corporation, USA).

Results and Discussion

Appearance and Optical Properties

All the studied films were flexible and translucent. The film's thickness was not modified with MMT addition ($p < 0.05$), but increased with the incorporation of CEO to the formulation up to 35 %. (Table 1). In particular, the films with CEO were more orange and brilliant than the ones without CEO, regardless of the MMT content. The optical properties of films (e. g., color and opacity) are also shown in Table 1. In nanocomposite films, with increasing MMT concentrations the luminosity slightly decreased (parameter *L* declines), while parameter *a* became progressively more negative and parameter *b* attained more positive values giving an overall tone tending toward the greenish-yellow. These shifts were accordingly reflected in the progressive increase in the parameter ΔE (color differential) with added amounts of clay in the formulation. The addition of CEO to protein films—without MMT—caused the same changes in color than those produced by incorporating the clay (parameters *L* and *a* decrease whereas *b* and ΔE

Table 1 Thickness, color parameters (*L*, *a*, *b*, ΔE), and opacity of soy protein isolate (SPI) films containing 0, 5 y 10 g of montmorillonite (MMT)/100 g SPI with or without clove essential oil (CEO)

Film	MMT (g/100 g SPI)	Thikness (μm)	Hunter-Lab color parameters				Opacity (UA mm^{-1})
			L	*a*	*b*	ΔE	
SPI	0	77.4 ± 5.9 [a]	92.13 ± 0.12 [c]	0.53 ± 0.01 [e]	1.79 ± 0.07 [a]	5.18 ± 0.12 [a]	2.25 ± 0.01 [c]
	5	73.2 ± 4.7 [a]	90.52 ± 0.24 [b]	0.05 ± 0.03 [b]	6.98 ± 0.37 [e]	8.59 ± 0.34 [c]	1.68 ± 0.03 [b]
	10	74.4 ± 6.3 [a]	89.98 ± 0.16 [a]	−0.09 ± 0.02 [a]	14.70 ± 0.47 [f]	14.92 ± 0.49 [d]	1.49 ± 0.03 [a]
SPI + CEO	0	104.0 ± 3.4 [b]	90.36 ± 0.14 [b]	0.05 ± 0.02 [b]	6.58 ± 0.22 [d]	8.48 ± 0.14 [c]	6.87 ± 0.01 [f]
	5	104.8 ± 4.9 [b]	91.96 ± 0.19 [c]	0.15 ± 0.02 [c]	3.52 ± 0.19 [c]	5.64 ± 0.17 [b]	6.56 ± 0.03 [e]
	10	100.1 ± 5.3 [b]	92.54 ± 0.07 [d]	0.41 ± 0.01 [d]	2.51 ± 0.03 [b]	4.84 ± 0.07 [a]	6.40 ± 0.03 [d]

Value for each film is the mean ± standard deviation. Values with different superscript letters are significantly different ($p < 0.05$) according to the Tukey test

increase), but when it was incorporated in nanocomposite systems the opposite effect was observed: parameters L and a became increase and b and ΔE decline (with less intensity when increasing MMT content. These opposite effects turned very similar color parameters between the protein film (SPI-0) and the ones containing clove essential oil and 10 g of MMT per 100 g of SPI (SPI + CEO-10).

As was previously reported (Echeverría, et al., 2014), the opacity of films decreased significantly by increasing the clay concentration, what would be consistent with a good degree of affinity between the soy proteins and the clay layers. According to Petersson and Oksman (2006) it could be assumed that MMT layers would be exfoliated in soy protein matrix in an important degree, as they suggest that the degree of exfoliation and volume fraction of the nanoreinforcement had a large influence on the transmittance of UV and visual light, and no reduction in the amount of light being transmitted through the nanocomposite films is an indication that the nanoreinforcements are fully exfoliated. The addition of CEO increased the opacity of films as it was reported in literature for lipid incorporation (Gontard et al., 1994; Quezada Gallo et al., 2000), according also with the significant increase of the film's thickness. This increment in opacity was higher in the presence of the nanoclay (3, 3.9, and 4.3 times for films with 0, 5 and 10 g MMT/100 g SPI, respectively). These results suggest a structural common effect between MMT and CEO, which would indicate some interactions between both components and consequently modifications in their interactions with the protein matrix.

Water Susceptibility

Table 2 shows the moisture content, water activity, solubility, and water vapor permeability of protein and nanocomposite films activated or not with CEO. The moisture content of protein films without and with CEO decreased significantly with the addition of clay (≅16 and 12 %, respectively), regardless of MMT concentration, and increased when CEO was incorporated in protein and nanocomposite films with 5 g/100 g SPI (≅15 and 20 %, respectively) despite the oily nature of this essential oil. Furthermore, in films with 10 g MMT/100 g SPI the lower effect on moisture content of clay was equilibrated with the increasing CEO one.

All the studied films showed a water activity lower than 0.6, suggesting that the microbial growth in them would be inhibited (Fennema, 1996). No differences in a_w were observed among protein and nanocomposite films, neither between protein films with and without CEO. Only when clay and CEO were added together a significantly decreased in a_w was observed respect to soy protein films. These results also suggest that the combined presence of MMT and CEO produce a distinct effect on the functionality of the resulting films. This lower value of a_w would indicate that water is preferably trapped in the matrix. Considering the oily nature of CEO, it may interact with the hydrophobic groups of proteins causing conformational changes, so the hydrophilic groups remain more available to retain water and also to interact with the clay. These conformational changes in protein structure would contribute to the significant increase in thickness. Furthermore, as a plasticizer, the presence of the essential oil may modify the degree of intercalation—exfoliation of the clay into the matrix, and consequently its ability to hold water.

Solubility is an important functional property in active films, so it can influence the release of the additives retained in the matrix indirectly (Papadokostaki & Petropoulos, 1998). Table 2 shows that the solubility of protein films in water decreased significantly with increasing clay concentration regardless of the presence of CEO. This effect of MMT on film solubility has been reported by other authors working with different biopolymers, and it was attributed to the formation of hydrogen bonds between the clay and the hydroxyl groups of these polymers (Almasi et al., 2010; Casariego, et al., 2009; Rhim et al., 2011). In a previous work (Echeverría, et al., 2014), a pronounced decline of soy protein solubilization in water was well established with the inclusion of MMT in the formulation, proving that the clay reduces the availability of free polypeptides in the film matrix. The addition of CEO only increased the solubility of films containing 10 g MMT/100 g SPI. Probably, the conformational changes in proteins could affect their ability to interact with water molecules, presumably by facilitating the progressive release of the active compound.

Table 2 Moisture content, water activity, water solubility and water vapor permeability (WVP) of soy protein isolate (SPI) films containing 0, 5 y 10 g montmorillonite (MMT)/100 g SPI with or without clove essential oil (CEO)

Film	MMT (g/100 g SPI)	Moisture content (%)	Water activity (a_w)	Water solubility (%)	WVP × 10^{-11} (g seg^{-1} m^{-1} Pa^{-1})
SPI	0	15.36 ± 0.19 ^{b}	0.565 ± 0.012 ^{b}	43.34 ± 0.25 ^{d}	6.75 ± 0.56 ^{b}
	5	13.49 ± 0.42 ^{a}	0.563 ± 0.011 ^{b}	42.11 ± 0.64 ^{c}	3.85 ± 0.25 ^{a}
	10	12.85 ± 0.12 ^{a}	0.535 ± 0.009 ^{b,d}	38.01 ± 0.47 ^{a}	2.92 ± 0.20 ^{a}
SPI + CEO	0	17.69 ± 0.66 ^{c}	0.541 ± 0.013 ^{b,d}	43.25 ± 0.03 ^{d}	5.76 ± 0.56 ^{b}
	5	16.26 ± 0.22 ^{b}	0.510 ± 0.014 ^{c,d,a}	42,28 ± 0.33 ^{c}	3.69 ± 0.31 ^{a}
	10	15.54 ± 0.03 ^{b}	0.495 ± 0.012 ^{a}	39.93 ± 0.90 ^{b}	2.97 ± 0.03 ^{a}

Value for each film is the mean ± standard deviation. Values with different superscript letters are significantly different ($p < 0.05$) according to the Tukey test

In contrast to these results, (Salgado, et al., 2013) observed that the activation of sunflower protein films with clove essential oil produce a decrease in film solubility. Meanwhile Gómez-Estaca, et al. (2010) found differences in solubility between gelatin and gelatin/chitosan films activated with the same essential oil, and suggested that these variations could determine differences in the biological activity of the films, related to the degree and rate of the active compounds release. In this regard, it could be assumed that the addition of clay—that reduced film's solubility—possibly would slow the release of active compounds, allowing to hold a remaining concentration of these molecules in the films over a longer period of time, and thus extending its effectiveness.

WVP values of soy protein films were similar to those reported for other protein films (Denavi et al., 2009; Gennadios et al., 1993; Maria Martelli et al., 2006; Mauri & Añón, 2006; Rhim et al., 2000; Salgado et al., 2013). The addition of clay to the formulation produced a significant drop in this property that was not dependent on the concentration of MMT. These decreases in the WVP is generally associated with a successful dispersion of the clay within the protein matrix, which distribution produced a more tortuous path for the passage of water molecules through the film, due to hydrophilic interactions between proteins and MMT, thus resulting in a lesser availability of the hydrophilic sites on the protein for the sorption of water molecules (Tunc, et al., 2007). (Echeverría, et al., 2014) evidenced that the diminution in WVP upon addition of the MMT to the soy protein matrix would be attributed to a decrease in both the water solubility coefficient and the diffusion of water throughout the film, with the latter effect being the more pronounced. Meanwhile, the addition of CEO to protein and nanocomposite films did not modify the WVP, despite its oily nature. This effect could be attributed to the good dispersion of the oil in these networks, as it is known that lipids generate a significant barrier to water vapor when they do form continuous phases. This behavior was also observed in sunflower protein films activated with clove essential oil (Salgado, et al., 2013) and in whey protein films added with oregano essential oil (Zinoviadou et al., 2009).

It is evident that the addition of clay to protein films contributes to reduce their water susceptibility, while the essential oil—despite its oily nature—cannot improve it.

Mechanical Properties

Mechanical properties of films are shown in Table 3. The addition of MMT to protein formulations produced a very important reinforcing effect, expressed in a significant increase in the tensile strength at break (σ_b) and Young's modulus (E), and a decrease in the elongation at break (ε_b). The addition of CEO to protein and nanocomposite formulations led the opposite effect, reducing σ_b and E, and increasing ε_b. Several authors have shown that some oils can act as plasticizers in protein films (Andreuccetti et al., 2009; Bertan et al., 2005), but others authors (Fabra et al., 2008) have reported that the effect on the mechanical properties depends on the lipid and the polymer used, and therefore the interactions between them. Similar effect on mechanical properties was reported by Azevedo et al. (2015) for nanocomposite films based on whey protein, montmorillonite, and citric acid.

It is worth noting that despite the plasticizing effect exerted by the clove oil, the addition of MMT caused a further strengthening effect in films containing CEO. So while nanocomposite films containing 10 g MMT/100 g SPI reached an increase of 105 and 200 % in σ_b and E, respectively, and a decrease of 340 % in ε_b, those that also contained CEO reached higher variations (230, 345, and 290 %, respectively). These results prove a lower plasticizing effect of clove essential oil with increasing clay concentration.

The notable improvement in the mechanical properties, especially with respect to Young's modulus in the nanocomposites films essentially results from the nature of the interaction between the soy proteins and the clay, with or without CEO addition. It has been reported that MMT and protein interactions could involve an interchange between the cationic groups of the amino-acid side chains (e.g., the $-NH_3^+$ moieties) and Na^+ ions occupying the sites of interaction on the MMT surface, and strong electrostatic interactions and hydrogen bonding occurring between the soy proteins and the highly unordered MMT layers within the film matrix (Ensminger

Table 3 Tensile strength and elongation at break (σ_b and ε_b) and Young's modulus (E) of soy protein isolate (SPI) films containing 0, 5, and 10 g of montmorillonite (MMT)/100 g SPI with or without clove essential oil (CEO)

CEO (ml/ g SPI)	MMT (g/100 g SPI)	σ_b [MPa]	ε_b [%]	E [MPa]
SPI	0	5.7 ± 0.3^{c}	42.3 ± 3.1^{d}	4.1 ± 0.3^{c}
	5	9.8 ± 0.5^{e}	31.2 ± 3.7^{c}	9.1 ± 0.8^{e}
	10	11.7 ± 0.5^{f}	9.6 ± 0.3^{a}	13.3 ± 0.6^{f}
SPI + CEO	0	2.5 ± 0.2^{a}	50.0 ± 3.3^{e}	1.1 ± 0.1^{a}
	5	4.4 ± 0.1^{b}	40.8 ± 1.2^{d}	2.5 ± 0.2^{b}
	10	8.2 ± 0.3^{d}	12.8 ± 0.5^{b}	4.9 ± 0.4^{d}

Value for each film is the mean ± standard deviation. Values in column with different superscript letters are significantly different ($p < 0.05$) according to the Tukey test

& Gieseking, 1939 and Ensminger and Gieseking, 1941). These interactions are critical for restraining the movement of the soy proteins, and that restriction is responsible for the majority of the resistance to traction in the form of a reinforcement of the modulus of elasticity of the nanocomposite films that in turn reduces the film's elongation under tensile stress. In addition, as moisture content in composite films is lower with MMT addition (Table 2), there is less water available to plasticize the protein matrix, and this effect contributes to the increase in Young's modulus, tensile strength, and lower elongation at break.

Morphology

X-ray diffraction and TEM studies were performed to analyze the degree of dispersion of MMT layers in the materials. Figure 1 shows the X-ray diffraction spectra of natural MMT plus the pure protein and MMT nanocomposite films with and without CEO. The sodium–MMT spectra shows its characteristic diffraction peak at around 2θ = 7, 2° corresponding to an interlaminar space of d_{001} = 1.2 nm (Ke & Stroeve, 2005). Soy protein films containing or not CEO showed no peaks in their spectra within the range analyzed, evidencing the amorphous nature of these films. In nanocomposite films, spectra without CEO, the characteristic peak of MMT was shifted to smaller angles generating two adjacent peaks. Peaks corresponding to nanocomposite films with 5 g MMT/100 g SPI appeared at 2.61° (d_{001} = 3.38 nm) and 2.02° (d_{001} = 4.37 nm) while those of films containg 10 g MMT/100 g SPI were at 3.24° (d_{001} = 2.72 nm) and 2.34° (d_{001} = 3.77 nm). These shifts would indicate the existence of structures with protein chains intercalated into the clay layers (Silvestre & Duraccio, 2011), being the interlayer

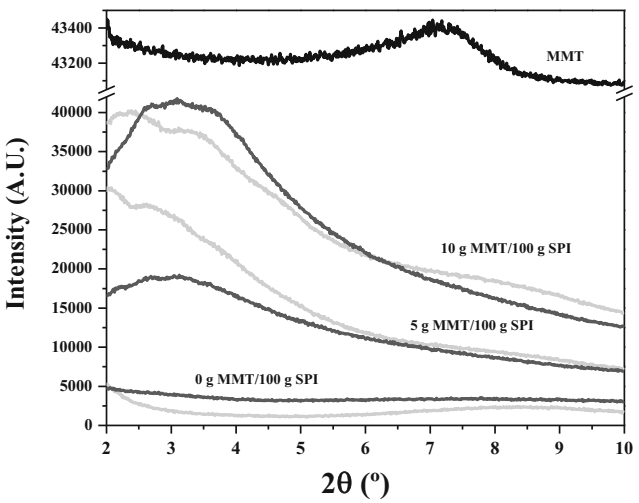

Fig. 1 X-ray–diffraction patterns of pure montmorillonite (MMT) (*black box*), soy protein isolate (SPI) films with 0, 5, and 10 g of MMT per 100 g of SPI, with (*grey box*) or without (*light gray box*) clove essential oil (CEO) addition

spacing of MMT lower for nanocomposite films with higher clay content. Tunç and Duman (2011) also reported a decrease in the interlaminar distance by increasing the concentration of clay. They attributed it to the clay dispersion process that became more difficult when the clay concentration in the filmogenic dispersion was increased. Nevertheless, for the two clay concentrations studied in this work, curves in the spectra rised as 2θ approaches 0°, providing evidence that these intercalated structures coexisted with exfoliated ones.

In the X-ray diffraction spectra of nanocomposite films with CEO, the characteristic peak of natural MMT was also shifted to lower angles and broadened. The peak for films containing 5 g MMT/100 g SPI has a maximum at 2θ = 3° which corresponds to an interlaminar distance d_{001} = 2.94 nm, and when this peak grows, it widens and shifts to higher angles with increasing clay concentration up to 10 g MMT/100 g SPI. While the spectra baseline falls sharply after the peaks, the intensity of the signal when approaching 2θ = 0° also gives evidence of the existence of exfoliated structures. These spectra demonstrates that the intercalated structures have lower interlaminar separations in the presence of CEO. Contrary to these results, Mascheroni, et al. (2010), reported that the addition of carvacrol to nanocomposite films based on whey protein and MMT caused an increase in the interlaminar distance of the clay, suggesting that the interaction between proteins and carvacrol favored protein intercalation between the clay layers. Furthermore, Park et al. (2008) reported that is expected a better retention of the active compounds in the polymer matrix if they obtain to intercalate between the clay layers. But the hydrophobic nature of clove oil suggests that the intercalation of phenolic compounds—mainly eugenol, gallic acid and caffeic acid—could be slightly favored among the interlaminar spaces of MMT.

Films were also studied by TEM in order to analyze the distribution of these nanostructures in the protein network. Figure 2 presents the microstructures of films containing 10 g MMT/100 g SPI, with and without the addition of CEO. They show the coexistence of intercalated and exfoliated structures, consistent with X-ray studies previously analyzed.

It is possible to affirm that the distribution of exfoliated layers of MMT seems to be more homogeneous in the presence of CEO than in its absence (Fig. 2c, d), despite being in a minus proportion as it was observed by X-ray diffraction studies (which showed a higher intensity of intercalated structures with a smaller interlaminar distance). Moreover, Fig. 2d shows in the denser and darker region that MMT is embedded in protein and CEO, proving that the three components were interacting among them, which explains the distinctive effect on some properties observed in nanocomposite films with CEO.

These evidences suggest that in these nanocomposite systems where the clay is highly exfoliated–intercalated in the

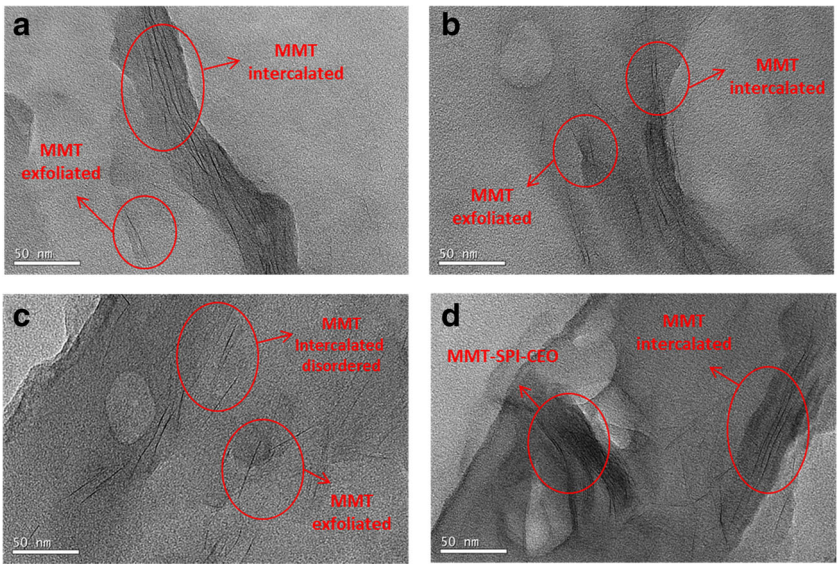

Fig. 2 Transmission electron microscopy (TEM) of nanocomposite films with 10 g montmorillonite (MMT)/100 g of soy protein isolate (SPI) without (**a**, **b**) and with clove essential oil (CEO) (**c**, **d**)

protein network, the release of the active compounds of CEO may be modified.

Antioxidant Properties

In vitro antioxidant properties of protein and nanocomposites films with and without CEO are shown in Table 4. Determinations were performed on the fraction of film that was dissolved in water, so that all samples have the same amount of active compounds, and differences in the antioxidant activity could be attributed to the release or not of these compounds, meaning they were more or less available to interact with the environment.

Soy protein films show a weak antioxidant activity, mainly attributable to polyphenolic compounds such as isoflavones; chlorogenic, caffeic, and ferulic acid—present in soy protein isolates, mostly glycosylated, and also to some extent to proteins or peptides derived from them (Pratt & Birac, 1979). The addition of 5 g MMT/100 g SPI to protein formulations did not modify significantly the antioxidant activity of films—determined by the ability to capture the ABTS radical and the reducing power of Fe (FRAP). But nanocomposite films with 10 g MMT/100 g SPI showed a significantly higher release of total phenols (about 3 times), suggesting that the intercalated–exfoliated MMT may facilitate the release of SPI polyphenols. These unexpected and promising results in the activation of soy isolate itself, suggest certain assumptions that future experiments should check. For example, salt ions of MMT could eventually interfere with any interaction between phenols and proteins, thus facilitating their release. In a different system, consisting of proteins, clove essential oil and sepiolite as clay, Giménez, et al. (2012) observed that the presence of sepiolite favored the gradual release of the phenolic compounds.

The addition of clove essential oil to the formulations activated protein and nanocomposite films with important antioxidant properties. This activity could be attributed to the phenolic compounds present in CEO, mainly eugenol, and gallic

Table 4 Antioxidant activity - determined by the ability to capture the ABTS radical and the reducing power of Fe (FRAP)- and total phenol release of soy protein (SPI) films with different content of montmorillonite (MMT), activated or not with clove essential oil (CEO)

Film	MMT (g/100 g SPI)	Antioxidant capacity		Total phenolic content *** (Folin-Ciocalteu)
		ABTS *	FRAP **	
SPI	0	18.7 ± 0.24^{a}	0.08 ± 0.01^{a}	9.8 ± 0.4^{a}
	5	18.2 ± 0.68^{a}	0.07 ± 0.01^{a}	7.2 ± 0.7^{a}
	10	34.9 ± 2.00^{b}	0.40 ± 0.04^{a}	28.7 ± 1.6^{b}
SPI + CEO	0	380.6 ± 11^{c}	6.41 ± 0.7^{b}	327.8 ± 8.4^{c}
	5	444.4 ± 35^{d}	6.64 ± 0.9^{b}	333.9 ± 3.2^{c}
	10	452.5 ± 11^{d}	6.59 ± 0.3^{b}	332.6 ± 7.7^{c}

*mg ascorbic acid/g soluble film; ** mmol $FeSO_4.7H_2O$ equivalents/g of soluble film; ***mg gallic acid/g soluble film

Value for each film is the mean ± standard deviation. Values in column with different superscript letters are significantly different ($p < 0.05$) according to the Tukey test

and cafeic acids (Dudonné et al., 2009). Only in determinations against $ABTS^+$ radical, nanocomposite films showed a higher antioxidant activity (at least 17 %) than protein ones, although the total phenolic content of these samples was similar ($p < 0.05$). The reducing effect determined by FRAP show no differences among protein and nanocomposite films. These results suggest that MMT induce polyphenols to be more reactive against radical scavenging, and that the presence of clay minerals did not modify the antioxidant properties of these compounds. It should be noted that total phenols measurement is not a direct measure of antioxidant activity. It is a complement; so, when it is compared to the activity, it is possible to speculate whether the observed effect is due to the concentration or to a greater or lesser antioxidant power. Considering that the solubility of films decreased with the addition of MMT, the greater or equal antioxidant activity exhibited by the nanocomposites respect to protein films—both with CEO—would strengthen the possibility that the presence of clay in these systems would favor the release of active compounds. This observation could be related with the significant increase of water solubility in the activated film at the highest MMT concentration (SPI-CEO-10) with respect to the film without CEO (Table 2).

These results induce to evaluate these films as a packaging material in a real system, since often interesting in vitro properties of films, are not replicable in real food systems because the active compounds are unable to be released. In this sense, considering that water is sometimes used as a food system model to determine the release of compounds, these results induce to evaluate applications in hydrophilic systems.

Antimicrobial Properties

Table 5 shows the antimicrobial activity in vitro of protein and nanocomposite films, with and without CEO. The addition of CEO to formulations conferred protein and nanocomposite films with good antimicrobial properties against different microorganisms, comparable to other published results (Gómez-

Table 5 Antimicrobial activity of soy protein isolate (SPI, 0 g MMT/100 g SPI) and nanocomposite films with 5 and 10 g de montmorillonite (MMT)/100 g de SPI, with and without clove essential oil (CEO) against different types of microorganisms

Microorganisms	% of inhibition					
	g MMT /100 g SPI without CEO			g MMT/100 g SPI with CEO		
	0	5	10	0	5	10
A. hydrophila CECT 839 T	19.7 ± 0.8^{a}	19.1 ± 0.8^{a}	18.9 ± 0.6^{a}	25.7 ± 0.6^{b}	29.8 ± 0.2^{c}	31.2 ± 1.5^{c}
A. niger CECT 2088	19.7 ± 0.8^{a}	20.4 ± 1.0^{a}	19.8 ± 0.6^{a}	41.5 ± 0.9^{b}	41.6 ± 1.1^{b}	40.7 ± 0.2^{b}
B. cereus CECT 148	23.0 ± 1.7^{b,d}	18.6 ± 0.6^{a}	19.5 ± 0.7^{a,b}	21.9 ± 0.7^{a,b}	29.4 ± 1.1^{c,d}	26.1 ± 0.2^{d}
B. coagulans CECT 561	20.1 ± 0.1^{b}	20.1 ± 0.2^{b}	18.7 ± 0.0^{a,c}	20.7 ± 0.1^{b}	19.8 ± 0.3^{b,c}	17.8 ± 0.5^{a}
B. animalis spp. lactis DSMZ 10140	19.0 ± 0.4^{a}	19.7 ± 0.0^{a}	19.1 ± 0.0^{a}	31.5 ± 0.2^{c}	32.9 ± 0.5^{d}	25.6 ± 0.1^{b}
B. thermosphacta CECT 847	18.9 ± 0.2^{a}	18.6 ± 0.4^{a}	18.2 ± 0.2^{a}	27.8 ± 0.1^{b}	31.7 ± 1.3^{c}	25.0 ± 1.6^{b}
C. freundii CECT 401	21.4 ± 0.6^{b}	19.1 ± 0.1^{a}	18.5 ± 0.0^{a}	29.3 ± 0.3^{c}	29.3 ± 0.2^{c}	30.5 ± 0.3^{c}
C. perfringens CECT 486	19.5 ± 0.6^{a}	18.8 ± 0.3^{a}	18.3 ± 0.1^{a}	32.3 ± 1.4^{b}	33.4 ± 0.8^{b}	19.2 ± 0.8^{a}
E. faecium DSM 20477	19.2 ± 1.1^{a}	18.7 ± 0.5^{a}	19.3 ± 2.0^{a}	20.6 ± 0.8^{a,b}	23.8 ± 0.9^{b}	21.9 ± 0.3^{a,b}
E. coli CECT 515	19.1 ± 0.8^{a,c}	18.6 ± 0.0^{a}	18.0 ± 0.0^{a}	22.2 ± 0.7^{b}	23.1 ± 0.8^{b}	21.0 ± 0.2^{b,c}
L. helveticus DSM 20075	22.0 ± 9.0^{a}	18.8 ± 0.1^{a}	17.7 ± 0.4^{a}	23.9 ± 0.3^{a}	23.8 ± 0.3^{a}	20.8 ± 0.3^{a}
L. innocua CECT 910	19.1 ± 0.2^{a}	19.1 ± 1.1^{a}	17.2 ± 1.0^{a}	17.2 ± 0.0^{a}	19.6 ± 0.2^{a}	18.8 ± 0.1^{a}
L. monocytogenes CECT 4032	18.6 ± 0.2^{a}	18.3 ± 0.0^{a}	17.7 ± 0.0^{a}	29.0 ± 0.1^{b}	32.7 ± 0.2^{b}	33.2 ± 3.1^{b}
P. expansum DSMZ 62841	19.5 ± 1.1^{a}	22.5 ± 0.3^{a}	20.2 ± 0.2^{a}	40.8 ± 1.7^{b}	50.0 ± 0.1^{c}	43.0 ± 0.5^{b}
P. phosphoreum CECT 4192	19.9 ± 0.6^{a}	20.1 ± 1.3^{a}	19.1 ± 0.8^{a}	43.6 ± 1.9^{c}	47.9 ± 1.5^{c}	30.0 ± 0.2^{b}
P. aeruginosa CECT 110	19.1 ± 0.1^{a}	20.6 ± 0.9^{b}	18.7 ± 0.1^{a}	26.7 ± 0.5^{c}	28.1 ± 0.3^{c}	21.2 ± 0.3^{b}
P. fluorescens CECT 4898	17.2 ± 0.2^{a}	21.4 ± 1.3^{a}	19.5 ± 0.4^{a}	28.8 ± 0.3^{a,b}	37.9 ± 0.4^{b}	24.0 ± 9.6^{a,b}
S. choleraesuis CECT 4300	21.5 ± 0.9^{b}	17.9 ± 0.5^{a}	18.6 ± 0.5^{a}	20.2 ± 0.5^{a,b}	20.5 ± 0.8^{a,b}	17.9 ± 0.6^{a}
S. putrefaciens CECT 5346 T	17.5 ± 0.3^{a}	19.6 ± 0.1^{a,b}	18.9 ± 0.5^{a,b}	29.9 ± 0.9^{d}	24.6 ± 0.8^{c}	20.2 ± 0.1^{b}
S. sonnei CECT 4887	20.7 ± 0.1^{b}	19.4 ± 0.3^{a,b}	18.6 ± 0.1^{a}	19.0 ± 0.4^{a}	18.9 ± 0.7^{a}	18.7 ± 0.1^{a}
S. aureus CECT 240	18.4 ± 0.2^{a,b}	19.4 ± 0.9^{b}	17.7 ± 0.1^{a}	24.0 ± 0.2^{d}	22.8 ± 0.1^{d}	19.5 ± 0.3^{b}
V. parahaemolyticus CECT 511 T	17.9 ± 0.4^{a,b}	18.7 ± 0.2^{b}	16.8 ± 0.8^{a}	39.3 ± 0.4^{d}	45.8 ± 0.4^{e}	34.0 ± 0.2^{c}
Y. enterocolitica CECT 4315	18.6 ± 0.2^{a,b}	17.5 ± 0.3^{a}	17.6 ± 0.1^{a}	26.2 ± 0.2^{c}	20.3 ± 0.5^{b}	26.2 ± 1.2^{c}

Value for each film is the mean ± standard deviation. Values with different superscript letters within the same line, are significantly different ($p < 0.05$) according to the Tukey test

Estaca, et al., 2010; Salgado, et al., 2013). The highest percentages of inhibition were for the molds *A. niger* and *P. expansum,* and for the Gram-negative bacteria *P. phosphoreum* and *V. parahaemolyticus* (Table 5). Ouattara et al. (1997) reported that the lipopolysaccharide nature of the cell wall of Gram-negative bacteria protect them against active compounds that could reach the cytoplasmic membrane; thus, Gram-positive bacteria were most sensitive to the action of essential oils. In this work, *S. choleraesuis* y *S. sonnei* bacteria were resistant to the effect of CEO, while other Gram-negative bacteria showed variable inhibitions. Among Gram-positive bacteria, only *B. coagulans* and *L. innocua* were not inhibited, showing a similar resistance to the Gram-negative ones. Gómez-Estaca, et al. (2010) observed the same effect. Differences in the resistance of Gram-positive bacteria against essential oils would be attributable to the variability among strains of the same species (Ouattara, et al., 1997). These results showed that soy protein films activated with CEO inhibited *S. putrefaciens* and *P. phosphoreum*, microorganisms involved in fish deterioration (López-Caballero et al., 2005). The sensitivity of these microorganisms to clove essential oil has been reported in the literature for both the pure oil and when it was incorporated into gelatin/chitosan or sunflower protein concentrate films (Gómez-Estaca, et al., 2010; Salgado, et al., 2013).

Comparing activated films together, the inhibition percentages of films varied differently with the addition of MMT depending on the microorganism. Although, in general, for sensitive microorganisms to clove essential oil, the percentage inhibition was independent of the presence or absence of MMT; in some cases the increased concentration of MMT appeared to reduce the inhibition zone (for example, *C. perfringens, P. phosphoreum and S. putrefaciens*), and in others appeared to increase it (for example, *A. hydrophila, B. cereus, L. monocytogenes* and *P. expansum*). Papadokostaki and Petropoulos (1998)reported that polymer structure would affect the release of the active components. Certainly, the diffusion of the different active compounds present in CEO may be modulated by the clay layers dispersed in the protein matrix. Even if any active molecule was intercalated into MMT layers, a selective release of the active compounds to the environment would occur.

In the literature, there are few studies that analyze the antimicrobial properties of nanocomposite films formed by protein–MMT with an added active agent. Mascheroni, et al. (2010) studied the activation of gluten–MMT films with carvacrol and reported a higher retention of the antimicrobial compound in the films due the interactions among proteins, MMT, and carvacrol. In this sense, nanocomposite films prepared with gelatine/egg white-sepiolite and clove essential oil favored the diffusion of the active compounds, but did not change their diffusion over time (Giménez, et al., 2012).

Sothornvit and Chollakup (2009) reported a bacteriostatic effect against *L. monocytogenes* for a whey protein/modified MMT system (without the addition of any other active compound), that was attributed to the action of the quaternary ammonium group of clay, which could break the membranes of cell wall causing the lysis of the bacteria. In the same work, this antimicrobial activity was tested using a natural MMT, but turned out to be zero. Even Hong and Rhim (2008) obtained the same result testing the natural MMT without being into a polymer matrix.

Mineral Release

The mineral released of nanocomposites films -determined by placing the materials in contact with water- was studied in order to assess if they diffuse and thus evaluate the potential use of these films as food packaging. Table 6 shows the content of the major minerals of MMT (Na, Mg, Al, and Si) in the aqueous fractions of films solubility tests. The presence of Na and Mg in these aqueous fractions seems not to come directly from the MMT as it was not observed a significant increase of these ions by incorporating the clay in the formulation. In the case of Mg, it is even seen a very slight but significant decrease in its release in films with 10 g MMT/100 g SPI, suggesting that clay—at this concentration—may act as a chelating of Mg naturally present in soy protein isolate. The addition of CEO contributed significantly to reduce the release of Mg to water, being this effect slightly more intense in the presence of MMT.

Conversely, although Al and Si were present in all films, those containing MMT released a greater amount of these ions

Table 6 Content of minerals (Na, Mg, Al, and Si) of soy protein isolate (SPI) and nanocomposites films with and without clove essential oil (CEO), obtained from the solubility in water of the films

Film	MMT (g/100 g SPI)	Na (mg/L)	Mg (mg/L)	Al (mg/L)	Si (mg/L)
SPI	0	112.0 ± 3.3^{a}	2.47 ± 0.04^{d}	0.018 ± 0.003^{ab}	0.16 ± 0.02^{a}
	5	113.0 ± 3.9^{a}	2.36 ± 0.01^{d}	0.035 ± 0.006^{c}	0.29 ± 0.04^{b}
	10	102.3 ± 6.5^{a}	2.07 ± 0.07^{cb}	0.039 ± 0.008^{c}	0.44 ± 0.02^{d}
SPI + CEO	0	109.9 ± 9.4^{a}	2.19 ± 0.11^{c}	0.010 ± 0.001^{a}	0.14 ± 0.01^{a}
	5	106.1 ± 2.9^{a}	1.90 ± 0.06^{ab}	0.032 ± 0.001^{cb}	0.29 ± 0.01^{b}
	10	117.1 ± 32^{a}	1.84 ± 0.03^{a}	0.029 ± 0.008^{cb}	0.37 ± 0.04^{c}

Value for each film is the mean ± standard deviation. In columns, Values with different superscript letters are significantly different ($p < 0.05$) according to the Tukey test

to water ($p < 0.05$). But only in the case of silicon this release was significantly dependent on MMT concentration. The presence of CEO slightly interfered the release of Si in films with 10 g MMT/100 g SPI, which supports that the clay interacted with proteins and the essential oil, which favored its dispersion in the film matrix with a high degree of exfoliation–intercalation.

These results suggest to evaluate the mineral release in nanocomposites based on clays in each condition of use, because if the minerals were able to diffuse to food, in certain concentrations they could become a health risk, or instead a benefit depending on the mineral and its chemical form. According to the European Food Safety Authority (EFSA, 2011) a package is considered safe if the aluminum silicate released into the food does not exceed the estimated intake of 1 mg per kg body weight per week. Furthermore, silicon in its bioavailable forms constitutes one of the essential minerals that provides more benefits to health. It seems to play a role in the bone mineralization and to participate in the atherosclerotic process, in addition to neutralize the neurotoxic effects of the aluminum (González Muñoz et al., 2009).

Conclusions

It was possible to activate nanocomposite films based on soy protein–montmorillonite with important antioxidant and antimicrobial properties through the addition of clove essential oil to the formulation. This essential oil exerted a plasticizing effect—reverse to the strengthening produced by the montmorillonite, verified in a decrease in the tensile strength at break and elastic modulus and an increase of the water content, without significantly affecting the elongation at break, water vapor permeability, and water solubility of the respective films. Finally, clove essential oil addition also favored the degree of exfoliation of the clay in the matrix, although in these systems coexist exfoliated and intercalated nanostructures.

These studies suggest the interactions among the three components of the film (soy protein), because some properties were differentially modified when both the clay and the essential oil were added to the protein formulation.

Presence appeared to facilitate the release of some active compounds and occasionally modify the antimicrobial activity of films as well as to release some of its Si and Al ions in contact with water. The ability of this nanoclay to modulate the release of active ingredients from protein arrays will be analyzed in future studies.

Acknowledgments The authors wish to thank the National Research Council (CONICET), the National Agency of Scientific and Technological Support (SECyT, PICT 2010-1837 and 2013-2124) and the Universidad Nacional de La Plata of Argentine (11/X618), and CYTED (309AC0382) for their financial support.

References

Almasi, H., Ghanbarzadeh, B., & Entezami, A. A. (2010). Physicochemical properties of starch-CMC-nanoclay biodegradable films. *International Journal of Biological Macromolecules, 46*(1), 1–5.

Andreuccetti, C., Carvalho, R. A., & Grosso, C. R. F. (2009). Effect of hydrophobic plasticizers on functional properties of gelatin-based films. *Food Research International, 42*(8), 1113–1121.

Arancibia, M., Alemán, A., López-Caballero, M. E., Gómez-Guillén, M. C., & Montero, P. (2015). Development of active films of chitosan isolated by mild extraction with added protein concentrates from shrimp waste. *Food Hydrocolloids, 43*, 91–99.

ASTM E96-00. (1996). Standard test methods for water vapor transmission of materials. In: Annual book of ASTM. Philadelphia, PA: USA.

Azevedo, V. M., Dias, M. V., Borges, S. B., Costa, A. L. C., Silva, E. K., Medeiros, E. A. A., & Soares, N. F. F. (2015). Development of whey protein isolate bio-nanocomposites: effect of montmorillonite and citric acid on structural, thermal, morphological and mechanical properties. *Food Hydrocolloids, 48*, 179–188.

Bertan, L. C., Tanada-Palmu, P. S., Siani, A. C., & Grosso, C. R. F. (2005). Effect of fatty acids and 'Brazilian elemi' on composite films based on gelatin. *Food Hydrocolloids, 19*(1), 73–82.

Cao, N., Fu, Y., & He, J. (2007). Preparation and physical properties of soy protein isolate and gelatin composite films. *Food Hydrocolloids, 21*(7), 1153–1162.

Casariego, A., Souza, B. W. S., Cerqueira, M. A., Teixeira, J. A., Cruz, L., Díaz, R., & Vicente, A. A. (2009). Chitosan/clay films' properties as affected by biopolymer and clay micro/nanoparticles' concentrations. *Food Hydrocolloids, 23*(7), 1895–1902.

Cressy, H. K., Jerrett, A. R., Osborne, C. M., & Bremer, P. J. (2003). A novel method for the reduction of numbers of *Listeria monocytogenes* cells by freezing in combination with an essential oil in bacteriological media. *Journal of Food Protection, 66*(3), 390–395.

Denavi, G., Tapia-Blácido, D. R., Añón, M. C., Sobral, P. J. A., Mauri, A. N., & Menegalli, F. C. (2009). Effects of drying conditions on some physical properties of soy protein films. *Journal of Food Engineering, 90*(3), 341–349.

Dudonné, S., Vitrac, X., Coutiére, P., Woillez, M., & Mérillon, J. M. (2009). Comparative study of antioxidant properties and total phenolic content of 30 plant extracts of industrial interest using DPPH, ABTS, FRAP, SOD, and ORAC assays. *Journal of Agricultural and Food Chemistry, 57*(5), 1768–1774.

Echeverría, I., Eisenberg, P., & Mauri, A. N. (2014). Nanocomposites films based on soy proteins and montmorillonite processed by casting. *Journal of Membrane Science, 449*, 15–26.

EFSA (2011). Scientific opinion on the safety evaluation of the substance, silver zeolite a (silver zinc sodium ammonium alumino silicate), silver content 2–5 %, for use in food contact materials. *EFSA Journal, 9*(2), 1999.

Ensminger, L. E., & Gieseking, J. E. (1939). The adsorption of proteins by montmorillonitic clays. *Soil Science, 48*(6), 467–474.

Ensminger, L. E., & Gieseking, J. E. (1941). The absorption of proteins by montmorillonitic clays and its effect on base-exchange capacity. *Soil Science, 51*(2), 125–132.

Fabra, M. J., Talens, P., & Chiralt, A. (2008). Tensile properties and water vapor permeability of sodium caseinate films containing oleic acid-beeswax mixtures. *Journal of Food Engineering, 85*(3), 393–400.

Fennema, O. R. (1996). Water and ice. In O. R. Fennema (Ed.), *Food chemistry (principles of food science series)* (pp. 18–95). New York: Marcel Dekker Inc..

Gennadios, A., Brandenburg, A. H., Weller, C. L., & Testin, R. F. (1993). Effect of pH on properties of wheat gluten and soy protein isolate

films. *Journal of Agricultural and Food Chemistry, 41*(11), 1835–1839.

Gennadios, A., McHugh, T. H., Weller, C. L., & Krochta, J. M. (1994). Edible coating and films based on protein. In *Edible coatings and films to improve food quality* (pp. 201–277). Lancaster, Pennsylvania: Technomic Publishing.

Giménez, B., Gómez-Guillén, M. C., López-Caballero, M. E., Gómez-Estaca, J., & Montero, P. (2012). Role of sepiolite in the release of active compounds from gelatin-egg white films. *Food Hydrocolloids, 27*(2), 475–486.

Gómez-Estaca, J., López de Lacey, A., López-Caballero, M. E., Gómez-Guillén, M. C., & Montero, P. (2010). Biodegradable gelatin-chitosan films incorporated with essential oils as antimicrobial agents for fish preservation. *Food Microbiology, 27*(7), 889–896.

Gontard, N., Duchez, C., Cuq, J. L., & Guilbert, S. (1994). Edible composite films of wheat gluten and lipids: water vapour permeability and other physical properties. *International Journal of Food Science and Technology, 29*, 39–50.

Gontard, N., Guilbert, S., & Cuq, J. L. (1993). Water and glycerol as plasticizers affect mechanical and water vapor barrier properties of an edible wheat gluten film. *Journal of Food Science, 58*(1), 206–211.

González Muñoz, M. J., Meseguer Soler, I., & Mateos Vega, C. J. (2009). Elementos ultratrazas ¿Nutrientes o tóxicos? *Revista de Toxicología, 26*(2–3), 93–103.

Gutierrez, J., Barry-Ryan, C., & Bourke, P. (2009). Antimicrobial activity of plant essential oils using food model media: efficacy, synergistic potential and interactions with food components. *Food Microbiology, 26*(2), 142–150.

Han, J. H., & Gennadios, A. (2005). Edible films and coatings: a review. In J. H. Han (Ed.), *Innovations in food packaging* (pp. 239–262). Oxford, England: Elsevier Academic Press.

Han, J. H., & Krochta, J. M. (2007). Physical properties of whey protein coating solutions and films containing antioxidants. *Journal of Food Science, 72*(5), E308–E314.

Hong, S. I., & Rhim, J. W. (2008). Antimicrobial activity of organically modified nano-clays. *Journal of Nanoscience and Nanotechnology, 8*(11), 5818–5824.

Ke, Y. C., & Stroeve, P. (2005). Chapter 1—background on polymer-layered silicate and silica nanocomposites. In Y. C. K. Stroeve (Ed.), *Polymer-layered silicate and silica nanocomposites* (pp. 1–67). Amsterdam: Elsevier Science.

Kong, F., Tang, J., Rasco, B., & Crapo, C. (2007). Kinetics of salmon quality changes during thermal processing. *Journal of Food Engineering, 83*(4), 510–520.

Kumar, P., Sandeep, K. P., Alavi, S., Truong, V. D., & Gorga, R. E. (2010). Preparation and characterization of bio-nanocomposite films based on soy protein isolate and montmorillonite using melt extrusion. *Journal of Food Engineering, 100*, 480–489.

Kuorwel, K. K., Cran, M. J., Sonneveld, K., Miltz, J., & Bigger, S. W. (2011). Antimicrobial activity of biodegradable polysaccharide and protein-based films containing active agents. *Journal of Food Science, 76*(3), 90–102.

López-Caballero, M. E., Gómez-Guillén, M. C., Pérez-Mateos, M., & Montero, P. (2005). A chitosan-gelatin blend as a coating for fish patties. *Food Hydrocolloids, 19*(2), 303–311.

Maria Martelli, S., Moore, G., Silva Paes, S., Gandolfo, C., & Laurindo, J. B. (2006). Influence of plasticizers on the water sorption isotherms and water vapor permeability of chicken feather keratin films. *LWT-Food Science and Technology, 39*(3), 292–301.

Mascheroni, E., Chalier, P., Gontard, N., & Gastaldi, E. (2010). Designing of a wheat gluten/montmorillonite based system as carvacrol carrier: rheological and structural properties. *Food Hydrocolloids, 24*(4), 406–413.

Mauri, A. N., & Añón, M. C. (2006). Effect of solution pH on solubility and some structural properties of soybean protein isolate films. *Journal of the Science of Food and Agriculture, 86*(7), 1064–1072.

Montreau, F. R. (1972). On the análisis of total phenolic compounds in wines by the Folin–Ciocalteau method. *Connaissance Vigne, 24*, 397–404.

Mytle, N., Anderson, G. L., Doyle, M. P., & Smith, M. A. (2006). Antimicrobial activity of clove (*Syzgium aromaticum*) oil in inhibiting *Listeria monocytogenes* on chicken frankfurters. *Food Control, 17*(2), 102–107.

Ouattara, B., Simard, R. E., Holley, R. A., Piette, G. J. P., & Bégin, A. (1997). Antibacterial activity of selected fatty acids and essential oils against six meat spoilage organisms. *International Journal of Food Microbiology, 37*(2–3), 155–162.

Papadokostaki, K. G., & Petropoulos, J. H. (1998). Kinetics of release of a model disperse dye from supersaturated cellulose acetate matrices. *Journal of Controlled Release, 54*(3), 251–264.

Park, J. K., Choy, Y. B., Oh, J. M., Kim, J. Y., Hwang, S. J., & Choy, J. H. (2008). Controlled release of donepezil intercalated in smectite clays. *International Journal of Pharmaceutics, 359*(1–2), 198–204.

Petersson, L., & Oksman, K. (2006). Biopolymer based nanocomposites: comparing layered silicates and microcrystalline cellulose as nanoreinforcement. *Composites Science and Technology, 66*(13), 2187–2196.

Pratt, D. E., & Birac, P. M. (1979). Source of antioxidant activity of soybeans and soy products. *Journal of Food Science, 44*(6), 1720–1722.

Pulido, R., Bravo, L., & Saura-Calixto, F. (2000). Antioxidant activity of dietary polyphenols as determined by a modified ferric reducing/antioxidant power assay. *Journal of Agricultural and Food Chemistry, 48*(8), 3396–3402.

Quezada Gallo, J. A., Debeaufort, F., Callegarin, F., & Voilley, A. (2000). Lipid hydrophobicity, physical state and distribution effects on the properties of emulsion-based edible films. *Journal of Membrane Science, 180*(1), 37–46.

Quilaqueo Gutiérrez, M., Echeverría, I., Ihl, M., Bifani, V., & Mauri, A. N. (2012). Carboxymethylcellulose-montmorillonite nanocomposite films activated with murta (*Ugni molinae Turcz*) leaves extract. *Carbohydrate Polymers, 87*(2), 1495–1502.

Re, R., Pellegrini, N., Proteggente, A., Pannala, A., Yang, M., & Rice-Evans, C. (1999). Antioxidant activity applying an improved ABTS radical cation decolorization assay. *Free Radical Biology and Medicine, 26*(9–10), 1231–1237.

Rhim, J. W., Gennadios, A., Handa, A., Weller, C. L., & Hanna, M. A. (2000). Solubility, tensile, and color properties of modified soy protein isolate films. *Journal of Agricultural and Food Chemistry, 48*(10), 4937–4941.

Rhim, J. W., Lee, S. B., & Hong, S. I. (2011). Preparation and characterization of agar/clay nanocomposite films: the effect of clay type. *Journal of Food Science, 76*(3), N40–N48.

Salgado, P. R., López-Caballero, M. E., Gómez-Guillén, M. C., Mauri, A. N., & Montero, M. P. (2013). Sunflower protein films incorporated with clove essential oil have potential application for the preservation of fish patties. *Food Hydrocolloids, 33*(1), 74–84.

Salgado, P. R., Ortiz, C. M., Musso, Y. S., Di Giorgio, L., & Mauri, A. N. (2015). Edible films and coatings containing bioactives. *Current Opinion in Food Science, 5*, 86–92.

Sánchez-González, L., Chiralt, A., González-Martínez, C., & Cháfer, M. (2011). Effect of essential oils on properties of film forming emulsions and films based on hydroxypropylmethylcellulose and chitosan. *Journal of Food Engineering, 105*(2), 246–253.

Sánchez-González, L., González-Martínez, C., & Chéfer, M. (2010). Physical and antimicrobial properties of chitosan-tea tree essential oil composite films. *Journal of Food Engineering, 98*(4), 443–452.

Seydim, A. C., & Sarikus, G. (2006). Antimicrobial activity of whey protein based edible films incorporated with oregano, rosemary and garlic essential oils. *Food Research International, 39*(5), 639–644.

Silvestre, C., Duraccio, D., & Cimmino, S. (2011). Food packaging based on polymer nanomaterials. Progress in Polymer Science (Oxford), 36(12), 1766–1782.

Sothornvit, R., & Chollakup, R. (2009). Properties of sericin-glucomannan composite films. *International Journal of Food Science and Technology, 44*(7), 1395–1400.

Sultanbawa, Y. (2011). Plant antimicrobials in food applications: Minireview. In A. Méndez-Vilas (Ed.), *Science against microbial pathogens: communicating current research and technological advances* (Vol. 2, pp. 1084–1093). Badajoz, Spain: Formatex Research Center.

Tunc, S., Angellier, H., Cahyana, Y., Chalier, P., Gontard, N., & Gastaldi, E. (2007). Functional properties of wheat gluten/montmorillonite nanocomposite films processed by casting. Journal of Membrane Science, 289(1–2), 159–168.

Tunç, S., & Duman, O. (2011). Preparation of active antimicrobial methyl cellulose/carvacrol/montmorillonite nanocomposite films and investigation of carvacrol release. *LWT - Food Science and Technology, 44*(2), 465–472.

Velluti, A., Sanchis, V., Ramos, A. J., Egido, J., & Marín, S. (2003). Inhibitory effect of cinnamon, clove, lemongrass, oregano and palmarose essential oils on growth and fumonisin B1 production by Fusarium proliferatum in maize grain. *International Journal of Food Microbiology, 89*(2–3), 145–154.

Yildirim, A., Mavi, A., Oktay, M., Kara, A. A., Algur, O. F., & Bilaloglu, V. (2000). Comparison of antioxidant and antimicrobial activities of Tilia (*Tilia argentea Desf ex DC*), sage (*Salvia triloba L.*), and black tea (*Camellia sinensis*) extracts. *Journal of Agricultural and Food Chemistry, 48*(10), 5030–5034.

Zinoviadou, K. G., Koutsoumanis, K. P., & Biliaderis, C. G. (2009). Physico-chemical properties of whey protein isolate films containing oregano oil and their antimicrobial action against spoilage flora of fresh beef. *Meat Science, 82*(3), 338–345.